Available online at www.sciencedirect.com
SCIENCE DIRECT®
Journal of Photochemistry and Photobiology A: Chemistry 162 (2004) 423–430
Journal of Photochemistry and Photobiology A:Chemistry
www.elsevier.com/locate/jphotochem

TiO_2-In_2O_3 photocatalysts: preparation, characterisations and activity for 2-chlorophenol degradation in water

D. Shchukin [a,c,*], S. Poznyak [b], A. Kulak [b], P. Pichat [c]

[a] *Institute for Micromanufacturing, Louisiana Tech University, 911 Hergot Avenue, Ruston, LA 71272, USA*
[b] *Belarusian State University, 220050 Minsk, Belarus*
[c] *Laboratoire "Photocatalyse, Catalyse et Environnement", CNRS UMR "IFoS", Ecole Centrale de Lyon, 69134, Ecully Cedex, France*

Received 29 May 2003; received in revised form 5 September 2003; accepted 10 September 2003

Abstract

Nanocrystalline bicomponent TiO_2–In_2O_3 powders with various Ti/In ratio have been prepared by the sol–gel technique and calcined at 473 and 723 K. Their crystalline structure, surface area, surface acidity, sorption properties with respect to 2-chlorophenol, and optical absorption were determined by appropriate techniques (XRD, BET, FTIR, and UV-Vis spectroscopies), while their photocatalytic activity (PCA) was tested in the case of the degradation of 2-chlorophenol in water. For both calcination temperatures, PCA increased with decreasing In_2O_3 contents reaching a maximum at ca. 10 wt.% of In_2O_3. For this latter sample and the one containing 20 wt.% In_2O_3, PCA was greatly enhanced with respect to TiO_2 especially for the samples pretreated at 473 K. The concentration of the main aromatic intermediate products (chlorohydroquinone and catechol) was considerably lower for TiO_2-In_2O_3 photocatalysts than for pure TiO_2. On the basis of various characterisations of the photocatalysts, the reasons invoked to explain the PCA enhancement due to In_2O_3 include a better separation of photogenerated charge carriers, an improved oxygen reduction and an increased surface acidity inducing a higher extent of adsorption of the aromatics.

Keywords: Titania; Nanocomposite; 2-Chlorophenol; Photodegradation; Indium oxide

1. Introduction

The photocatalytic degradation of organic compounds is investigated as a means of purifying water [1–7]. In particular, chlorophenols constitute an important class of water pollutants. Human activities, such as water disinfection, waste incineration and uncontrolled use of herbicides, are the major sources of chlorophenols in the environment [8].

Photocatalytic degradation has been studied with semiconductor suspensions and particulate thin films immobilised on a substrate. Titanium dioxide is currently considered as the most promising photocatalyst because of its absence of toxicity, reasonable photocatalytic activity, relatively low cost, and high stability toward photocorrosion. Numerous efforts have been made to improve the photocatalytic properties of titanium dioxide. It has been shown that the modification of TiO_2 by inorganic ions, metal particles, dyes or addition of another semiconductor can enhance or lower the photocatalytic activity. In particular, a number of researchers have reported that titania particles coupled with other inorganic oxides and sulfides such as SiO_2 [9–13], Al_2O_3 [10], ZrO_2 [11,14], SnO_2 [15–17], WO_3 [18–21], MoO_3 [20,21], V_2O_5 [22], CdS [23–25], rare earth oxides [26], Fe_2O_3 [27], can change the photocatalytic efficiency. Moreover, an extension of the energy range of photoexcitation may be observed in such systems [23,24,27].

The present work focuses on the photocatalytic properties of coupled TiO_2–In_2O_3 nanostructured powders prepared by the sol–gel technique. These catalysts were tested in the photocatalytic degradation of 2-chlorophenol (2-CP). The influence of the In_2O_3 content on the photocatalytic activity, surface area, surface acidity, optical absorption, oxygen reduction and other characteristics of the photocatalysts has been investigated.

2. Experimental

2.1. Preparation of the photocatalysts

TiO_2, In_2O_3 and TiO_2–In_2O_3 nanostructured photocatalysts were prepared by the sol–gel technique. Indium(III) nitrate and $TiCl_4$ were used as precursors. To obtain

* Corresponding author. Tel.: +1-318-257-5144; fax: +1-318-257-5104.
E-mail address: shchukin@latech.edu (D. Shchukin).

1010-6030/$ – see front matter © 2004 Elsevier B.V. All rights reserved.
doi:10.1016/S1010-6030(03)00386-1

In_2O_3 sol, a 12% NH_4OH solution was added dropwise to 0.25 mol l^{-1} aqueous $In(NO_3)_3$ under continuous stirring at 273 K till the pH was about 8. The precipitate thus obtained was washed thoroughly with distilled water until no NO_3^- ions were detected in the supernatant. Then, after addition of a small amount of concentrated HNO_3 used as a stabiliser, the precipitate was ultrasonically treated to obtain a transparent stable indium hydroxide sol (120–130 g l^{-1}, particle size 4–6 nm). Hydrous TiO_2 sol was prepared in similar way as previously described in detail [28].

To fabricate composite TiO_2-In_2O_3 catalysts, In_2O_3 and TiO_2 sols were mixed in a definite proportion and dried under reduced pressure at room temperature. Then the obtained xerogels were annealed in air at 473 or 723 K for 2 h.

Thin films of the oxides were deposited onto a quartz substrate by spin coating and then heated at 473 K for 20 min. This procedure was repeated several times to achieve 100 nm film thickness. The films were subsequently calcined in air at an appropriate temperature for 2 h.

2.2. Photocatalytic activity measurements

A cylindrical flask of ca. 90 ml equipped with a bottom optical window of ca. 4 cm in diameter was used as a photoreactor. The suspension in the photoreactor was magnetically stirred. The irradiation was provided by a Philips HPK high-pressure Hg lamp (125 W) through a 2.2 cm thick circulating water cell (to avoid heating the suspension by IR radiation) and a cutoff filter ($\lambda > 340$ nm, Corning 0.52). The radiant flux entering the photoreactor was 40 mW cm^{-2}; the corresponding number of photons per second potentially absorbable by the TiO_2 was ca. 1.3×10^{17}. All photocatalytic experiments were performed at near-room temperature.

Suspensions containing 2 g l^{-1} of photocatalyst and 10^{-3} mol l^{-1} of 2-CP (Aldrich) were usually used in the photocatalytic activity measurements. The aerated suspension was stirred in the dark for 90 min before irradiation to achieve adsorption equilibrium of 2-CP. The concentrations of 2-CP and its aromatic intermediate products were measured by HPLC using a LDC/Milton Roy system comprising a Constametric 3000 isocratic pump and a Spectro Monitor D UV detector adjusted at 254 nm. A reverse-phase column, 25 cm long, 4.6 mm i.d., packed with Spherisorb 5 ODS2, was used. The mobile phase was a mixture of methanol (35 (vol.%/vol.%)), deionized doubly distilled water (55 (vol.%/vol.%)), and acetonitrile. Identification of the eluting compounds was made by comparing their retention times to those of commercial compounds purchased from Aldrich.

2.3. Characterisation measurements

X-ray powder diffraction patterns of the photocatalysts were obtained using a HZG 4A powder diffractometer (Carl Zeiss, Jena) with Co Kα radiation (Mn filter). The average crystallite size was estimated from the X-ray line broadening according to Scherrer's equation. Optical transmission and absorption spectra of the films were measured using a Cary 500 UV-Vis-NIR spectrometer (Varian).

The surface area of the catalyst powders was determined by the BET method using a Micromeretics Gemini II 2375 Surface Area Analyzer. Before measurement, the samples were outgassed at 423 K for 12 h. The adsorbate was N_2.

IR absorbance spectra were measured with a resolution of 1 cm^{-1} using a Perkin-Elmer Spectrum 1 FTIR spectrometer. Before the measurements, 2-CP was adsorbed on the surface of the samples from pure liquid 2-CP and then the samples were dried at 353 K in an air flow for 3 h to remove physically adsorbed 2-CP.

Electrochemical measurements were carried out in a standard two-compartment three-electrode cell with a platinum counter-electrode and an Ag|AgCl|KCl (saturated) electrode as the reference electrode (+0.201 V versus SHE). All potentials were determined with respect to this reference electrode and controlled by a conventional potentiostat with a programmer. The counter-electrode compartment was separated from the working electrode by a fine glass frit. The electrochemical measurements were made at room temperature in 0.1 mol l^{-1} NaOH solution prepared using doubly distilled water and analytical-grade NaOH.

3. Results and discussion

3.1. XRD and BET measurements

XRD analysis showed that the TiO_2, In_2O_3, and TiO_2–In_2O_3 materials annealed at 473 and 723 K consisted of only two crystalline phases: anatase and cubic In_2O_3 (Fig. 1). Annealing at temperatures up to 1073 K resulted in the appearance of rutile but no Ti–In mixed phase was detected, indicating the absence of significant chemical interaction between the oxides in this temperature range. The broadening of all the peaks indicated that the TiO_2 and In_2O_3 crystalline domains had a diameter smaller than 30 nm. In the mixed oxides, the size of both TiO_2 and In_2O_3 crystallites was smaller than in the pure oxides. Thus, in the pure oxide powders annealed at 723 K, the average crystallite size was 10 nm for TiO_2 and 20 nm for In_2O_3, whereas in the binary oxide samples (TiO_2(50)–In_2O_3(50)) the average size was only 5 nm for TiO_2 and 17 nm for In_2O_3. Moreover, the addition of In_2O_3 to titania inhibited the anatase-to-rutile transformation which in the pure TiO_2 begins at 743–773 K, whereas in the TiO_2–In_2O_3 composites, traces of rutile appeared only at 973 K. The above-mentioned phenomena are often observed in composite TiO_2-based materials and are associated with the increased separation of the TiO_2 domains as the fraction of the other phase increases [9–13,19,26].

The BET surface areas of the TiO_2-In_2O_3 materials are indicated in Table 1. The binary oxide powders have an enhanced surface area in comparison with the pure oxides, which is consistent with the decreasing average crystallite

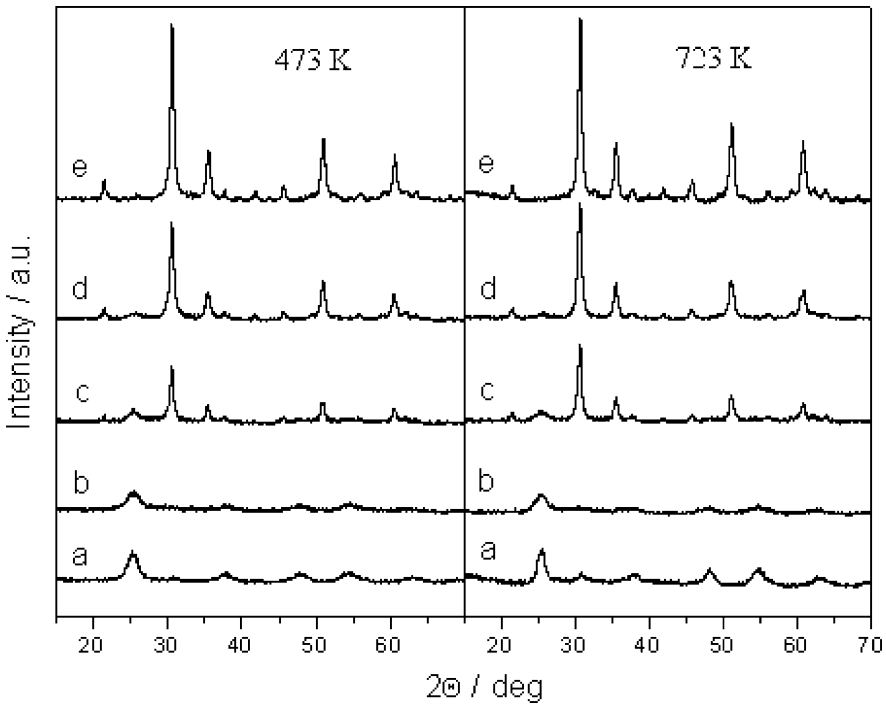

Fig. 1. X-ray diffractograms of TiO_2, In_2O_3 and TiO_2–In_2O_3 powders annealed at 473 and 723 K: (a) TiO_2 100 wt.%; (b) TiO_2 75 wt.%–In_2O_3 25 wt.%; (c) TiO_2 50 wt.%–In_2O_3 50 wt.%; (d) TiO_2 25 wt.%–In_2O_3 75 wt.%; (e) In_2O_3 100 wt.%.

size in the composites. As expected, the surface area decreased during the annealing treatment. It differed only slightly according to the TiO_2:In_2O_3 ratio.

3.2. FTIR study of surface acidity

Since a correlation between the surface acidity of catalysts and their photocatalytic activity has been previously shown [11,20,29], we examined the surface acidity of the TiO_2–In_2O_3 powders by the adsorption of pyridine (Pyr) and the use of FTIR spectrometry. Employing Pyr as a probe molecule to characterise surface acidity is well-documented since long ago [30–33]. Particularly, the Pyr vibration modes in the 1400–1650 cm^{-1} region [34] are informative.

The FTIR spectra recorded after adsorption of Pyr on the pure oxide samples and the TiO_2(50)–In_2O_3(50) composite are shown in Fig. 2. The spectrum of free Pyr is also presented for comparison. In accordance with previous data [31–33], the bands at 1444, 1492, and 1605 cm^{-1} observed for pure TiO_2 catalyst can be assigned to Pyr coordinated to Lewis-acid surface sites. The 19b mode at 1444 cm^{-1} is the strongest for TiO_2. Two bands corresponding to this mode overlap in the case of In_2O_3 powders. This indicates the existence of two kinds of Lewis-acid sites on the indium oxide surface. Characteristically, the shift of the bands at 1436 and 1596 cm^{-1} for non-adsorbed Pyr is higher for Pyr adsorbed on In_2O_3 than on TiO_2, which allows one to conclude that In_2O_3 has stronger acid sites. Because the bands at 1444 and

Table 1
Surface area ($m^2\ g^{-1}$) of the TiO_2–In_2O_3 powders annealed at different temperatures

Sample	Annealing temperature	
	473 K	723 K
TiO_2(100)	213	65
TiO_2(90)–In_2O_3(10)	230	71
TiO_2(75)–In_2O_3(25)	228	71
TiO_2(50)–In_2O_3(50)	222	72
TiO_2(25)–In_2O_3(75)	200	68
In_2O_3(100)	122	39

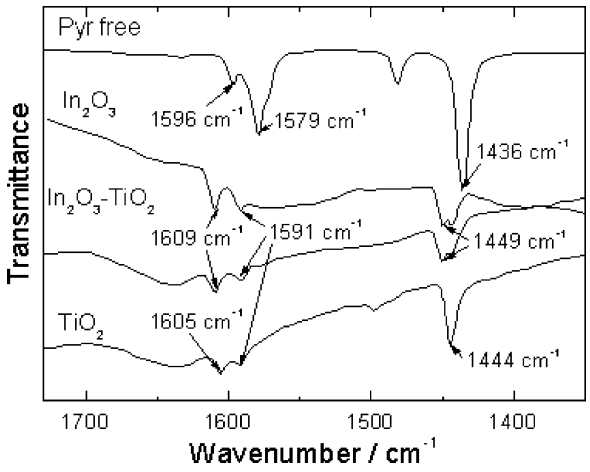

Fig. 2. FTIR spectra of TiO_2, In_2O_3 and TiO_2–In_2O_3 powders after adsorption of pyridine and spectrum of free pyridine.

1591 cm^{-1} exist for Pyr adsorbed on both TiO_2 and In_2O_3, and because the bands at 1605 and 1609 cm^{-1} overlap, the spectrum of Pyr adsorbed on TiO_2(50)–In_2O_3(50) did not differ noticeably from that of Pyr adsorbed on In_2O_3. In all cases, bands at ca. 1544 and 1638 cm^{-1} typical of pyridinium ions, that is, Pyr adsorbed on Bronsted acid sites, were not detected.

3.3. FTIR study of 2-CP adsorption

Since the affinity of the catalyst surface for reactant species should be regarded as an important factor for photocatalytic degradation efficiency, we studied the adsorption of 2-CP on the TiO_2 and In_2O_3 samples using the FTIR technique (Fig. 3). The oxide samples were exposed to rather low amounts of 2-CP to limit the quantity of non-adsorbed 2-CP. Assignment of the 2-CP IR bands was made according to reported data [35,36]. The OH bending vibrations of 2-CP were almost absent after the adsorption, indicating that the 2-CP OH group likely interacted with the solid oxide surface. Similar results have been previously found for 2-CP adsorption on Al_2O_3 and Fe_2O_3 [35] and for 4-chlorophenol adsorbed on TiO_2 Degussa P-25 [37]. For 2-CP adsorbed on In_2O_3, the bands at 832 and 745 cm^{-1} corresponding to Cl-sensitive vibrations were significantly shifted in comparison with those of non-adsorbed 2-CP (Fig. 3). This observation suggests that the interaction of 2-CP with the In_2O_3 surface affects the Cl atom. That is consistent with the existence of stronger Lewis acid sites on In_2O_3 compared with TiO_2; the electronegative Cl atom would play a role analogous to that of the nitrogen atom of Pyr.

In short, the FTIR study shows that 2-CP interacts with the oxides via its OH group, and the Cl atom is also perturbed by the adsorption especially in the case of In_2O_3.

3.4. Photocatalytic activity for 2-CP removal. Origins of the In_2O_3 effect

The photocatalytic activity of the prepared catalysts for the decomposition of 2-CP was investigated for the powders annealed at 473 and 723 K. Fig. 4(a) shows the change in 2-CP concentration as a function of irradiation time for the pure oxides and the most active composite annealed at 473 K. These kinetic curves can be approximated as a pseudo-first-order process which allowed us to determine the rate constant (k) and thus to quantitatively compare the efficiencies of the different catalysts under similar experimental conditions (Fig. 4b). For both calcination temperatures, k increased with decreasing In_2O_3 contents reaching a maximum at ca. 10 wt.% of In_2O_3. For this latter sample and the one containing 20 wt.% In_2O_3, k was greatly enhanced with respect to TiO_2 especially for the samples pretreated at 473 K. In contrast to pure TiO_2, pure In_2O_3 and the binary oxides had a lower photocatalytic activity when annealed at higher temperature (Fig. 4b). This effect can be partly associated with the decrease in surface area as the annealing temperature increases (Table 1); nevertheless, a similar decrease in pure TiO_2 surface area led to a slight increase in activity. Moreover, this explanation cannot be used to

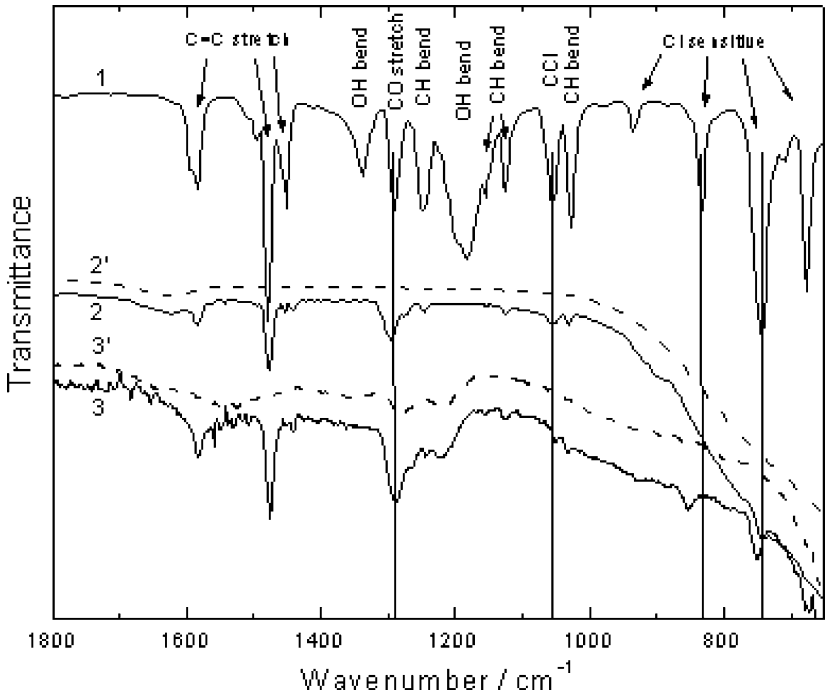

Fig. 3. FTIR spectra of TiO_2 (2, 2′) and In_2O_3 (3, 3′) samples recorded before (2′, 3′) and after (2, 3) adsorption of 2-CP. For reference, spectrum (1) corresponding to a condensed 2-CP phase is included.

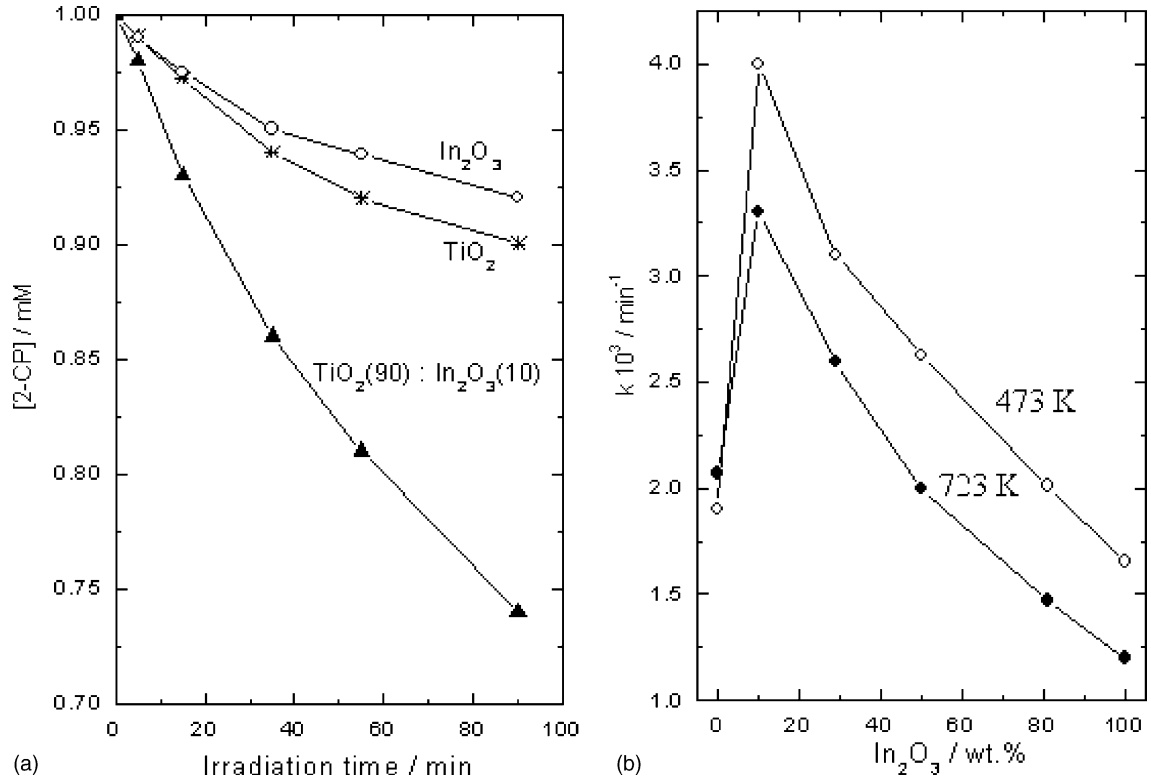

Fig. 4. (a) Plots of 2-CP concentration as a function of irradiation time for TiO_2, In_2O_3 and $TiO_2(90)$–$In_2O_3(10)$ photocatalysts annealed at 473 K; (b) initial rate constants for the samples annealed at 473 and 723 K as a function of In_2O_3 content.

interpret the dependence of k on the In_2O_3 content because the binary oxide powders with different composition possess approximately similar specific surface area and other factors should be taken into consideration.

Since TiO_2 and In_2O_3 differently absorb UV light, the photocatalytic activity could also be affected by a change in photon harvesting depending on the solid composition. To clarify this point, thin films of the photocatalysts under investigation were prepared on a quartz substrate and their UV-Vis absorption spectra were recorded in the 250–700 nm range. The absorption edge regions of these spectra for the TiO_2, In_2O_3 and $TiO_2(50)$–$In_2O_3(50)$ films are shown in Fig. 5. There is a blue shift of the absorption edge of the composite films compared to that of TiO_2. The origin of this

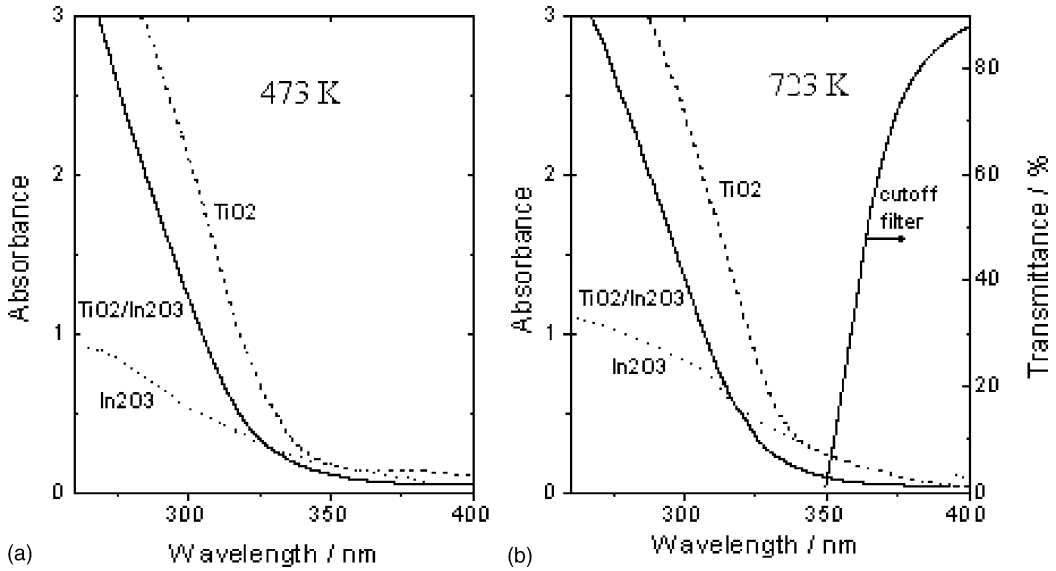

Fig. 5. Absorption spectra of $TiO_2(50)$–$In_2O_3(50)$ composite films as well as one-component TiO_2 and In_2O_3 films annealed at (a) 473 K and (b) 723 K. For comparison, the transmission spectrum of the cutoff filter used in the 2-CP photodegradation experiments is also shown.

shift has been considered previously [39]. Here it is important to emphasise that the composite materials absorb less photons in comparison with one-component materials when using a cutoff filter with $\lambda > 340$ nm (the transmittance spectrum of this filter is also shown in Fig. 5). Therefore, the 2-CP removal rate constant normalized to the absorbed light would even be greater for the TiO_2–In_2O_3 composites.

A number of researchers have shown that mixing different semiconductors with appropriate energy levels can produce a more efficient photocatalyst owing to the better separation of photogenerated charge carriers [15–19,23–25,38]. Two of us have previously shown [39] that nanocrystalline TiO_2 and In_2O_3 films, prepared from colloids identical to those used in this work, have similar band gaps, but different flat band potentials. Therefore, the conduction band electrons photogenerated in the TiO_2 nanoparticles can transfer to the lower lying conduction band of In_2O_3 while photogenerated holes move in the opposite direction. Such improvement of the charge separation may account for the enhanced photocatalytic activity of the TiO_2-In_2O_3 composites. In addition, we have carried out electrochemical experiments employing TiO_2 and In_2O_3 nanoparticulate film electrodes to compare the catalytic activity of these semiconductors for O_2 reduction. Fig. 7 presents dark current versus potential curves recorded with these electrodes in O_2-saturated solutions containing an indifferent electrolyte (0.1 mol l^{-1} NaOH). Molecular oxygen is reduced on the In_2O_3 surface at a markedly lower overvoltage than on the TiO_2 surface. These results allow us to suggest that mixing TiO_2 with In_2O_3 is beneficial not only for charge carrier separation but also for accelerating the associated transfer of photogenerated electrons to O_2. It has been documented [40–42] that the O_2 reduction by trapped electrons on the TiO_2 surface is a rate-limiting step of the photocatalytic oxidation of organic compounds.

Another possible explanation of the increased photocatalytic activity of the composites may stem from the change in surface acidity. Our FTIR results have indeed shown that the surface of In_2O_3-containing powders has an enhanced acidity compared with that of TiO_2. The importance of surface acidity is in line with previous conclusions [43].

3.5. Variations in the concentrations of chlorohydroquinone and catechol versus In_2O_3 content

Analysis of the primary intermediate products of 2-CP degradation may provide an additional insight into the degradation pathways and mechanism. Chlorohydroquinone (CHQ) and catechol (CAT) are the major aromatic intermediate products in UV-irradiated TiO_2 aqueous suspensions containing 2-CP as the initial pollutant [44]. Fig. 6 presents the concentrations of CHQ and CAT normalized to the concentration of 2-CP having disappeared as a function of the In_2O_3 content. The use of pure In_2O_3 and the binary oxide samples as photocatalysts resulted in lower normalized concentration of CHQ and CAT in comparison with pure TiO_2. This tends to suggest that these more hydroxylated compounds having rings with a higher electron density are more easily retained on or near the photocatalyst surface—owing to In_2O_3—and thereby more rapidly transformed. The easier reduction of O_2 deduced from the electrochemical measurements (Fig. 7) can also be invoked because it should enhance the concentration of superoxide prone to react with the radical-cations formed from CHQ and CAT [45]. A priori this in line with the FTIR spectra of Pyr indicating the presence of stronger Lewis acid sites which are electron-accepting sites. Not surprisingly, the sum of normalized concentrations of CHQ and CAT was minimal for the TiO_2(90)–In_2O_3(10) composite which exhibited the highest photocatalytic activity. Another result

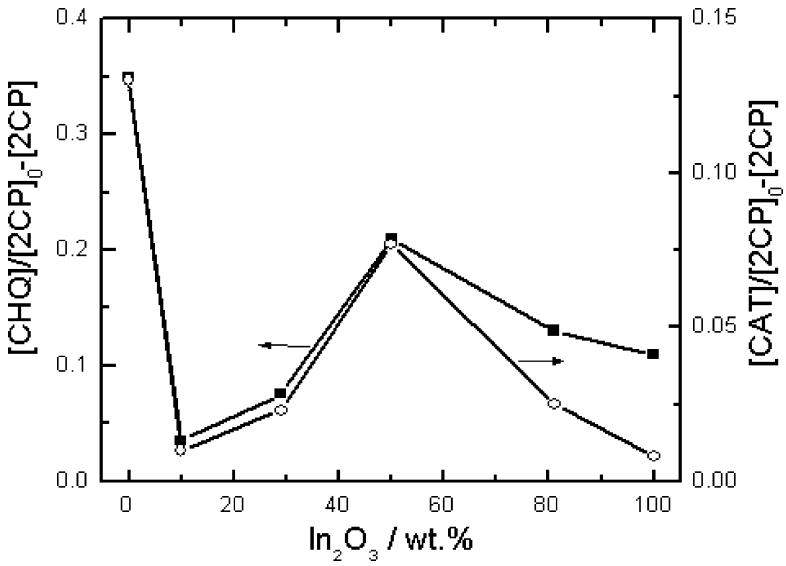

Fig. 6. Plots of the chlorohydroquinone (CHQ) and catechol (CAT) concentrations normalized to the concentration of photodestructed 2-CP as a function of the In_2O_3 content. The concentrations were measured after photocatalytic degradation of 2-CP for 90 min.

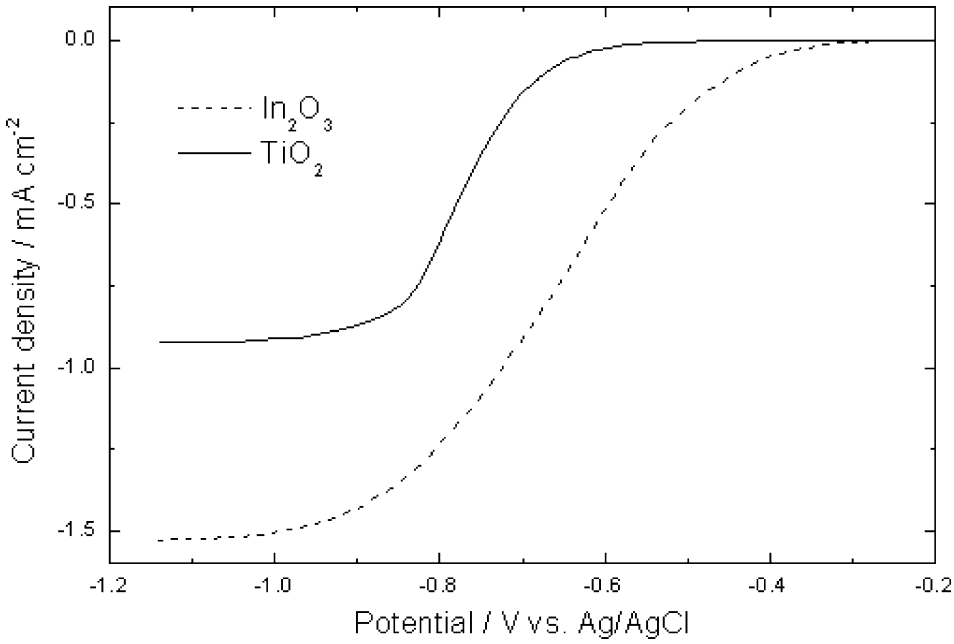

Fig. 7. Potentiodynamic voltammograms of TiO_2 and In_2O_3 thin film electrodes annealed at 723 K. Electrolyte: oxygen-saturated 0.1 mol l^{-1} NaOH solution stirred with a magnetic stirrer. Potential sweep rate: 5 mV s^{-1}.

shown in Fig. 6 is that the concentrations of CHQ and CAT were about equal except for the samples containing 80 and 100% of In_2O_3 for which the concentration in CAT was lower than that in CHQ. This result is consistent with the fact that, as inferred from the FTIR spectra, the interaction of 2-CP with In_2O_3 affects the Cl atom and can therefore make the removal of this atom easier.

4. Conclusions

This study shows that modification of TiO_2 with In_2O_3 can produce more active photocatalysts, at least for the removal of 2-CP (or analogs) for which a maximum increase in the activity by a factor of about two relative to TiO_2 was observed. This increase is not linked to an increase in surface area or to an absorption augmentation in the near-UV spectral region. It stems from changes in both bulk and surface properties which we have tried to identify. In line with other investigations, our study incites one to further explore the coupling of TiO_2 with other stable semiconductors, taking into account the suggested origins of the enhanced photocatalytic activity as guidelines. The preparation method should achieve an intimate solid mixture to render easier the exchange of reactants, intermediate products and active species between the solid phases.

Acknowledgements

D.G.S acknowledges support from INTAS (Grant YSF 00–161) which, in particular, allowed him to carry out the degradation and FTIR experiments in Lyon.

References

[1] M. Schiavello (Ed.), Photocatalysis and Environment, Kluwer Academic Publishers, Dordrecht, 1988.
[2] D.F. Ollis, H. Al-Ekabi (Eds.), Photocatalytic Purification and Treatment of Water and Air, Elsevier, Amsterdam, 1993.
[3] M.A. Fox, M.T. Dulay, Chem. Rev. 93 (1993) 341.
[4] P. Pichat, in: M.A. Tarr (Ed.), Chemical Degradation for Wastes and Pollutants: Environmental and Industrial Applications, Marcel Dekker, New York, 2003, pp. 77–119.
[5] M.R. Hoffmann, S.T. Martin, W. Choi, D.W. Bahnemann, Chem. Rev. 95 (1995) 69.
[6] A. Mills, S. Le Hunte, J. Photochem. Photobiol. A 108 (1997) 1.
[7] A. Fujishima, K. Hashimoto, T. Watanabe, TiO_2 Photocatalysis, BKC, Tokyo, 1999.
[8] K.R. Krijgsheld, A. van der Gen, Chemosphere 15 (1986) 825.
[9] Z. Liu, R.J. Davis, J. Phys. Chem. 98 (1994) 1253.
[10] C. Anderson, A.J. Bard, J. Phys. Chem. B 101 (1997) 2611.
[11] X. Fu, L.A. Clark, Q. Yang, M.A. Anderson, Environ. Sci. Technol. 30 (1996) 647.
[12] L.J. Alemany, M.A. Banares, E. Pardo, F. Martin, M. Galan-Fereres, J.M. Blasco, Appl. Catal. B: Environ. 13 (1997) 289.
[13] K.Y. Jung, S.B. Park, Appl. Catal. B: Environ. 25 (2000) 249.
[14] S.P. Fen, G.W. Meng, L.D. Zhang, Chin. Sci. Bull. 43 (1998) 1613.
[15] K. Vinodgopal, P.V. Kamat, Environ. Sci. Technol. 29 (1995) 841.
[16] K. Vinodgopal, I. Bedja, P.V. Kamat, Chem. Mater. 8 (1996) 2180.
[17] Y. Cao, X. Zhang, W. Yang, H. Du, Y. Bai, T. Li, J. Yao, Chem. Mater. 12 (2000) 3445.
[18] Y.R. Do, W. Lee, K. Dwight, A. Wold, J. Solid State Chem. 108 (1994) 198.
[19] G. Marci, L. Palmisano, A. Sclafani, A.M. Venezia, R. Campostrini, G. Carturan, C. Martin, V. Rives, G. Solana, J. Chem. Soc., Faraday Trans. 92 (1996) 819.
[20] J. Papp, S. Soled, K. Dwight, A. Wold, Chem. Mater. 6 (1994) 496.
[21] S. Dube, N.N. Rao, J. Photochem. Photobiol. A: Chem. 93 (1996) 71.
[22] S.T. Martin, C.L. Morrison, M.R. Hoffmann, J. Phys. Chem. 98 (1994) 13695.

[23] L. Spanhel, H. Weller, A. Henglein, J. Am. Chem. Soc. 109 (1987) 6632.
[24] K.R. Gopias, M. Bohorquez, P.V. Kamat, J. Phys. Chem. 94 (1990) 6435.
[25] R.A. Doong, C.H. Chen, R.A. Maithreepala, S.M. Chang, Water Res. 35 (2001) 2873.
[26] J. Lin, J.C. Yu, J. Photochem. Photobiol. A: Chem. 116 (1998) 63.
[27] D. Bockelmann, R. Goslich, D. Bahnemann, in: M. Backer, K.-H. Funken, G. Schneider (Eds.), Solar Thermal Energy Utilization, vol. 6, Springer-Verlag GmbH, Heidelberg, 1992, p. 397.
[28] S.K. Poznyak, A.I. Kokorin, A.I. Kulak, J. Electroanal. Chem. 442 (1998) 99.
[29] K. Shibata, T. Kiyoura, J. Kitagawa, T. Sumiyoshi, K. Tanabe, Bull. Chem. Soc. Jpn. 46 (1973) 2985.
[30] H. Knozinger, Adv. Catal. 25 (1976) 184.
[31] C. Morterra, S. Coluccia, A. Chiorino, F. Boccuzzi, J. Catal. 54 (1978) 348.
[32] C. Morterra, G. Ghiotti, E. Garrone, J. Chem Soc., Faraday Trans. I 76 (1980) 2102.
[33] P. Pichat, M.-V. Mathieu, B. Imelik, Bull. Soc. Chim. Fr. 8 (1969) 2611.
[34] C.H. Kline Jr., J. Turkevich, J. Chem. Phys. 12 (1944) 300.
[35] K.-H.S. Kung, M.B. McBride, Environ. Sci. Technol. 25 (1991) 702.
[36] The Aldrich Library of Infrared Spectra, third ed., Aldrich Chemical Co., 1981.
[37] U. Stafford, K.A. Gray, P.V. Kamat, A. Varma, Chem. Phys. Lett. 205 (1993) 55.
[38] Y. Cao, X. Zhang, W. Yang, H. Du, Y. Bai, T. Li, J. Yao, Chem. Mater. 12 (2000) 3445.
[39] S.K. Poznyak, D.V. Talapin, A.I. Kulak, J. Phys. Chem. B 105 (2001) 4816.
[40] H. Gerischer, Electrochim. Acta 38 (1993) 3.
[41] H. Gerischer, A. Heller, J. Electrochem. Soc. 139 (1992) 113.
[42] C.M. Wang, A. Heller, H. Gerischer, J. Am. Chem. Soc. 114 (1992) 5230.
[43] P. Pichat, M.-N. Mozzanega, H. Courbon, J. Chem. Soc., Faraday Trans. I 83 (1987) 697.
[44] J.-C. D'Oliveira, G. Al-Sayyed, P. Pichat, Environ. Sci. Technol. 24 (1990) 990.
[45] L. Cermenati, P. Pichat, C. Guillard, A. Albini, J. Phys. Chem. 101 (1997) 2650.